ACS Sustainable Chemistry & Engineering

pubs.acs.org/journal/ascecg

Research Article

Arsenic Toxicity: Carbonate's Counteraction Revealed

Swathy Jakka Ravindran, Shantha Kumar Jenifer, Jayashree Balasubramanyam, Sourav Kanti Jana, Subramanian Krishnakumar, Sailaja Elchuri, Ligy Philip, and Thalappil Pradeep*

Cite This: *ACS Sustainable Chem. Eng.* 2020, 8, 5067−5075

Read Online

ACCESS | Metrics & More | Article Recommendations | Supporting Information

ABSTRACT: Well-known purification technologies built for arsenic (As) removal from drinking water are not sustainable, either being unaffordable or inefficient in the elimination of traces of As. In our experiments, we observed that carbonate ion can counteract the effects of As exposure as it efficiently prevented As-induced cytotoxicity on epithelial cell lines of the small intestine (IEC-6). The cotreatment of IEC-6 cells with 40 ppm of carbonates and As (≥3 ppm) showed substantial remissions in the As-induced cytotoxicity and increased the viability from 50% to 75%. The production of intracellular reactive oxygen species (ROS) and cellular acidification were also reduced in this process (pH increase from 5 to 6.5). Thus, the present study suggests that the cytoprotective effect of carbonate can involve multiple pathways, such as reduction of extracellular/intracellular acidosis, H_2O_2 decomposition, balancing mitochondrial potential, and immobilization of As. We show that As-contaminated drinking water enriched with carbonates up to 40 ppm has a reduced toxic effect on cells in comparison to that of an As-alone sample. Therefore, carbonates can act as an adjunct in addition to the prevailing approaches to tackle mass poisoning by As. We believe that this study is initial evidence for developing an alternative method to tackle the prevailing mass environmental poisoning by As, using locally available, affordable, safe, and sustainable solutions.

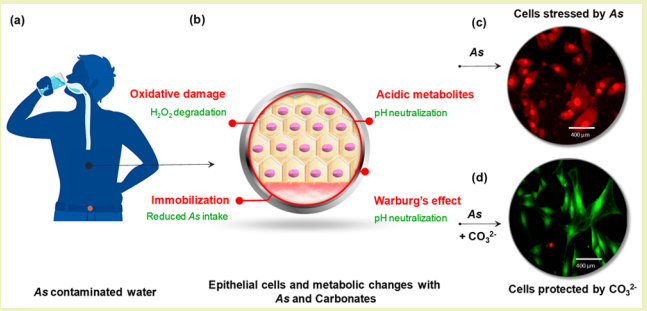

KEYWORDS: *Arsenic toxicity, Cytoprotection, Carbonates in water, Counteraction, Toxicity mitigation*

Downloaded via INDIAN INST OF TECH MADRAS on May 10, 2020 at 16:42:04 (UTC).
See https://pubs.acs.org/sharingguidelines for options on how to legitimately share published articles.

INTRODUCTION

While arsenic (As) ranks first in the priority list of hazardous substances,[1,2] over 150 million people in 70 countries are estimated to be exposed to unsafe levels of As in drinking water globally.[3,4] In India, it is estimated that about 70.4 million people in 20 states are at risk due to the presence of excess amounts of As in groundwater.[5] With these startling numbers, As poisoning is regarded as the "worst mass poisoning in history". Thus, intense efforts are taken to reduce As exposure to humans. Most of the water purification plants designed for As removal are failing to reduce below the maximum safe level (10 μg/L) insisted by the World Health Organization (WHO).[6−8] The cost and energy associated with membrane processing, ion exchange, and adsorption techniques are high while they deliver poor performance and introduce toxic substances, creating secondary pollution.[9−11] Chemical reagents such as chlorine and ozone are used in the oxidation of As^{3+} to As^{5+}, a widely used As removal technique.[11] Nanomaterials are increasingly researched upon[12] and applied in the field[13] to solve As contamination.[14] Interventional research to alleviate As toxicity is in its early stages and is of unknown effectiveness.[15] In the following, we present the problem of As poisoning and essential background necessary to appreciate this work.

Arsenic: Toxicity, Oxidative Stress, and Human Disease. Arsenic in water provides the majority of its daily dose through inorganic As species (As^{3+} and As^{5+}) that enter orally. Among the two forms, As^{3+} and As^{5+}, As exists primarily as As^{5+} in water under aerobic conditions.[16] Thus, the effect of carbonate on As^{5+} in water was studied in this work. It has been observed that when some of the vital human metabolic pathways are stressed by As, progressive cellular dysfunction results in apoptosis and diverse health effects such as cancer and cardiovascular diseases are manifested.[17−21] It inhibits glucose uptake by cells, oxidation of fatty acids, gluconeogenesis, and further production of acetyl CoA. Experimental evidence shows that the acute toxicity of As is due to the development of a superoxide anion radical ($O_2^{\bullet-}$), singlet oxygen ($^1O_2$), peroxide radical ($ROO^{\bullet}$), hydroxyl radical ($^{\bullet}OH$), dimethylarsenic radical [$(CH_3)_2As^{\bullet}$], oxidant-induced DNA damage, and hydrogen peroxide (H_2O_2).[22] Arsenic

Received: November 16, 2019
Revised: March 12, 2020
Published: March 17, 2020

ACS Publications

© 2020 American Chemical Society

https://dx.doi.org/10.1021/acssuschemeng.9b06850
ACS Sustainable Chem. Eng. 2020, 8, 5067−5075

exposure leads to an increase in levels of reactive oxygen species (ROS) and reactive nitrogen species produced, which can surpass the antioxidant capacity of the living cells.[23,24] Additionally, the morphology and the integrity of mitochondria are disturbed by As and a rapid decline in the mitochondrial membrane potential occurs. Acidification of growth media that contained cultured cell lines exposed to As at levels below the lethal concentrations has been observed in this work. A possible reason for this increased extracellular acidification is lactate production, generated as a result of the Warburg effect (aerobic glycolysis).[23,25]

Carbonate's Association with As and its Toxicity. A broad range of associations have been encountered in the literature between carbonate and various As species.[26] Arsenic discharges from the aquifer rocks into groundwater are strongly related to the concentration of bicarbonate in the leaching solution.[7,27] This release is mainly because of the formation of arseno−carbonate complexes, which are stable in groundwater.[26] In the case of the worm *Caenorhabditis elegans*, the gene *abts-1*, which encodes a sodium (Na^+)-dependent Cl^-/HCO_3^- transporter (a bicarbonate transporter), has been reported to protect it from As toxicity. Stronger expression of the *abts-1* gene was observed in the cells of *C. elegans* after exposure to As, and the cells of the worms lacking *abts-1* were found to be hypersensitive to As.[28] In the experiments performed by Ruby et al., the dissolution of As in a stomach environment was found to be strongly pH dependent and the extent of dissolution was observed to decrease by 16% when there was a minimal increase in pH.[29] Arsenic-affected cells produce acidic metabolites and undergo the Warburg effect, an effect also seen in cancer cells.[30] In the case of cancer cells, this acidification is generally treated with systemic buffers and carbonates that can significantly inhibit the development of metastases.[30,31] In the As-affected cells, ROS are the major reason for the intensification of As toxicity, and prior research implies that the carbonate (or bicarbonate) anion has a role in promoting peroxide decomposition, found to be nine times faster than sodium hydroxide.[32] Intracellular pH is a crucial factor that regulates cellular behavior. In the presence of oxygen, pyruvate is imported into mitochondria for the Krebs (or tricarboxylic acid) cycle and oxidative phosphorylation in the cells.[33] Under anaerobic conditions, glucose is converted into pyruvate followed by its transformation into lactate to cope with the low oxygen availability. For unascertained reasons, even during stressed conditions, like As exposure or cancer, cells perform glycolysis, irrespective of oxygen availability. This is termed as the Warburg effect, and it involves the increased uptake of glucose and higher lactate production, shifting the pH of the microenvironment toward an acidic range.[25] At such stressed conditions, aerobic glycolysis is inefficient in generating adenosine 5′-triphosphate (ATP) and its advantage to the cells is unclear.[25]

Sustainable Counteraction for As Toxicity. From the discussion above, it is clear that the carbonate anion can counteract the potential risk of As toxicity, following any or all of the possible routes. Here, we have investigated the hypothesis that the increased systemic concentrations of carbonate species can reduce various cellular dysfunctions, namely, extracellular/intracellular acidosis, H_2O_2 decomposition, balancing mitochondrial potential, and immobilization of As into the cell. Since the majority of As present in water is absorbed in the gastrointestinal tract (ingestion) and causes a cascade of cellular dysfunctions, our study was performed using epithelial cell lines of the small intestine (IEC-6).

Even though H_2O_2 is not a free radical, it is next to superoxide anion and hydroxyl radical in its toxic effects, which is a key member in the class of ROS. Earlier reports state that increased cellular concentrations of free iron (during overload of iron in the organism) imposes deleterious effects where Fe(II) participates during the decomposition of H_2O_2, known as a Fenton reaction, which generates reactive hydroxyl radicals.[34] Through CV experiments, it was observed that carbonates can reduce the H_2O_2 produced by As-exposed cells by 95%.

Following an initial observation of rapid acidification in the culture media that contained As-exposed cells, we show that the buffering capacity of carbonates can regulate the impact of cellular acidification caused by As. The current study shows that the administration of safe levels of carbonate in the form of sodium carbonate or calcium carbonate can counteract the toxicity levels of As. As bolus ingestion of bicarbonates can also lead to metabolic disturbances, we propose that a divided dose of carbonate-balanced water containing sodium carbonate and/or calcium carbonate throughout the day is the best way to compensate the impact of As on human body.

As the chemistry of ions present in the groundwater is complex[35−37] and As-related cellular changes are diverse, this paper stands as a piece of salient preliminary evidence to tackle the mass poisoning due to As, using abundantly available carbonates. The addition of carbonates does not involve complex chemicals or need energy, as may be necessary for the currently practiced arsenic removal techniques, and thus it can contribute to developing a sustainable and effective method for As remediation.

MATERIALS AND METHODS

Cell Culture. Rat small intestinal cells (IEC-6) obtained from National Centre for Cell Science (NCCS, Pune, India) were maintained in Dulbecco's modified Eagles medium (DMEM) supplemented with 10% fetal bovine serum and secured with antibiotics, namely, penicillin and streptomycin (100 IU/100 μg). IEC-6 intestinal cells were grown in T-75 culture flasks and were maintained at 37 °C at a 5% CO_2 atmosphere. Upon reaching confluency, the growth medium from the T-75 culture flask was removed and the cells were gently rinsed with 2 mL of phosphate buffered saline (PBS), and then 5 mL of trypsin-EDTA (ethylenediaminetetraacetic acid) solution was added and kept at room temperature (in a laminar hood) for 40 s. Then, the trypsin-EDTA solution was removed and the flask was kept at 37 °C in a CO_2 incubator for 3 min, and the cells were detached completely from the surface by tapping gently over the flask. The cells were then suspended in a fresh growth medium and then transferred to sterile T-75 flasks. The total volume was made up to 5 mL using the growth medium.

Cell Viability Assay. The viability of the cells was assessed by a MTT [3-(4, 5-dimethylthiazol-2-yl)-2,5-diphenyltetrazolium bromide tetrazolium] assay.[38] About 5×10^3 cells were plated in 96-well plates with DMEM containing 10% FBS (fetal bovine serum). The cells were incubated for 24 h under 5% CO_2 and 95% O_2 at 37 °C. Then the DMEM with FBS was removed and replaced with a serum-free medium. Arsenic and carbonate were given to cells through the DMEM media, and the system was incubated for 24 h. After treatment, the medium was removed and replaced with 500 μL of 0.5% MTT containing DMEM and then incubated at 37 °C for 4 h. After incubation, the MTT containing medium was removed from the plate and 500 μL of dimethyl sulfoxide was added and mixed well, and after 2h, the color that developed was read at 570 nm in a microplate spectrophotometer (SpectraMax M5Microplate Reader). The un-

https://dx.doi.org/10.1021/acssuschemeng.9b06850
ACS Sustainable Chem. Eng. 2020, 8, 5067−5075

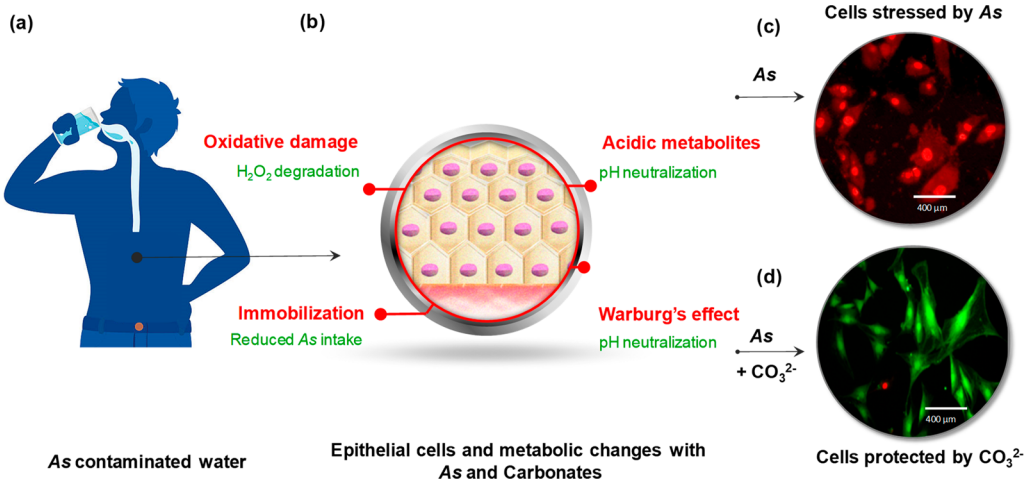

Figure 1. Schematic representation of As-induced toxic metabolism and carbonate's cytoprotective action to encounter them.

treated control cells were used for the normalization of absorbance to calculate the changes in cell viability. The cell viability was calculated as the percentage of viable cells and then plotted against time in hours. The total As concentration of the cells was estimated using inductively coupled plasma mass spectrometry (ICP-MS) (PerkinElmer Nex ION 300 ICP-MS).

Cellular Morphology. The morphological changes in the cells due to As exposure and the cytoprotective action of As^{5+} and carbonate were studied under a phase-contrast microscope (EVOS FL auto cell imaging system).

Live/Dead Staining. A LIVE/DEAD viability/cytotoxicity kit designed for mammalian cells (Molecular Probes, Invitrogen) was used for differentiating live cells from dead cells. The treated adherent cells, cultured on 24-well plates as confluent monolayers, were washed with 500−1000 volumes of Dulbecco's phosphate-buffered saline (D-PBS) prior to the assay to remove serum, growth media, and other ions added during the studies. About 20 μL/10 mL of ethidium homodimer-1 stock solution and 5 μL/10 mL of calcein were mixed thoroughly, and the mixture was added directly to cells. Imaging was performed at an excitation/emission wavelength of 494/517 nm for calcein and at 528/617 nm for ethidium homodimer-1 using an EVOS FL auto cell imaging system.

Determination of ROS. 2′,7′-dichlorodihydrofluorescein diacetate (H_2DCFDA) (Molecular Probes, Eugene, OR) is a nonfluorescent dye that is oxidized by intracellular ROS to form highly fluorescent 2′,7′-dichlorofluorescein. The cells, after treatment with different concentrations of ions, were washed once with DMEM, stained with 20 μM H_2DCFDA, and incubated at 37 °C for 30 min. The dye was then removed, and the cells were washed with DMEM. Fluorescence images were taken at 485 nm excitation and 535 nm emission using the EVOS FL auto cell imaging system.

Cyclic Voltammetry. Cyclic voltammetry (CV) experiments were performed using an electrochemical analyzer (CHI 600A) to study the H_2O_2 decomposition caused by $CaCO_3$ and Na_2CO_3. For CV experiments, a precleaned gold (Au) electrode was chosen as a working electrode, Ag/AgCl was chosen as the reference electrode, and Pt was fixed as the counter electrode. Arsenic-treated cells were separated from the growth media, suspended, and lysed in PBS (pH ∼ 7). H_2O_2 produced by the As-treated cells lysed in PBS was exposed to various concentrations of $CaCO_3$ during voltammetry measurements. This sample was used for H_2O_2 measurement. CV measurements for every sample were performed in a potential window between 0 to +1.2 V with a fixed scan rate of 100 mV s^{-1} at room temperature. For reference values, CV profiles of Au were performed in a blank solution (only PBS).

Cellular pH Profiling. A stock of a pH indicator solution containing 100 mM bromothymol blue (BTB) was prepared in water with 10 mL of 4% sodium hydroxide and 20 mL of absolute alcohol. For the pH profiling of cells through staining, the cell culture medium was first aspirated and then the washing procedure was completed three times using PBS. Following this step, the cells were treated with the pH indicator solution (1 mg/mL) and removed after 10 min of incubation. Finally, the redundant pH indicator stain sticking to the extracellular lines of the cells were washed using 20% aqueous ethanol solution for three times. Treated cells were observed under the bright field EVOS FL auto cell imaging system.

RESULTS AND DISCUSSION

The cause and development of As toxicity are complex and have not been fully understood. A cascade of cellular dysfunction occurs in which oxidative stress plays a vital role. The oxidative damage further leads to loss of mitochondrial membrane potential, which complicates the toxicity, leading to cell death. Figure 1 is a schematic representation of As-induced toxic metabolism resulting from the exposure to As contaminated water (Figure 1a) and carbonate's cytoprotective action to counter it. In the present study, a model of rat intestinal cells, IEC-6 in confluent culture, was used. Important analytical studies, namely, cell viability, morphological changes, cell death, ROS generation, H_2O_2 decomposition, As uptake, and cellular pH neutralization, were performed to understand the role of the carbonate ion. Figure 1b shows vital cellular dysfunction as a result of As intake and the carbonate's activity to encounter each of them. Part c and d of Figure 1 represent the cells stressed by As toxicity and the carbonates' cytoprotective action against it.

Qualitative Assessment of Carbonate's Cytoprotective Action. It has been reported that As intake leads to a decrease in the efficacy of cellular defense mechanisms (reduced glutathione), and it increases the formation of superoxide derived free radicals. This leads to progressive cellular dysfunction, leading to apoptosis.[21] IEC-6 cells upon treatment with varying concentrations of As^{5+}, namely, 1, 3, and 5 ppm for 24 h, resulted in a 50% loss of cell viability at 3 and 5 ppm As exposure. At concentrations of As lower than 1 ppm, a longer incubation time was required to achieve cell death with As. In such cases, it was difficult to differentiate natural vs arsenic-induced cell death. The cell viability was studied by differentiating live cells vs dead cells through staining with calcein and ethidium bromide, followed by fluorescence imaging. The intracellular esterase present in live cells hydrolyzes the acetomethoxy group of nonfluorescent calcein AM dye, making it fluorescent. Ethidium bromide is a

https://dx.doi.org/10.1021/acssuschemeng.9b06850
ACS Sustainable Chem. Eng. 2020, 8, 5067−5075

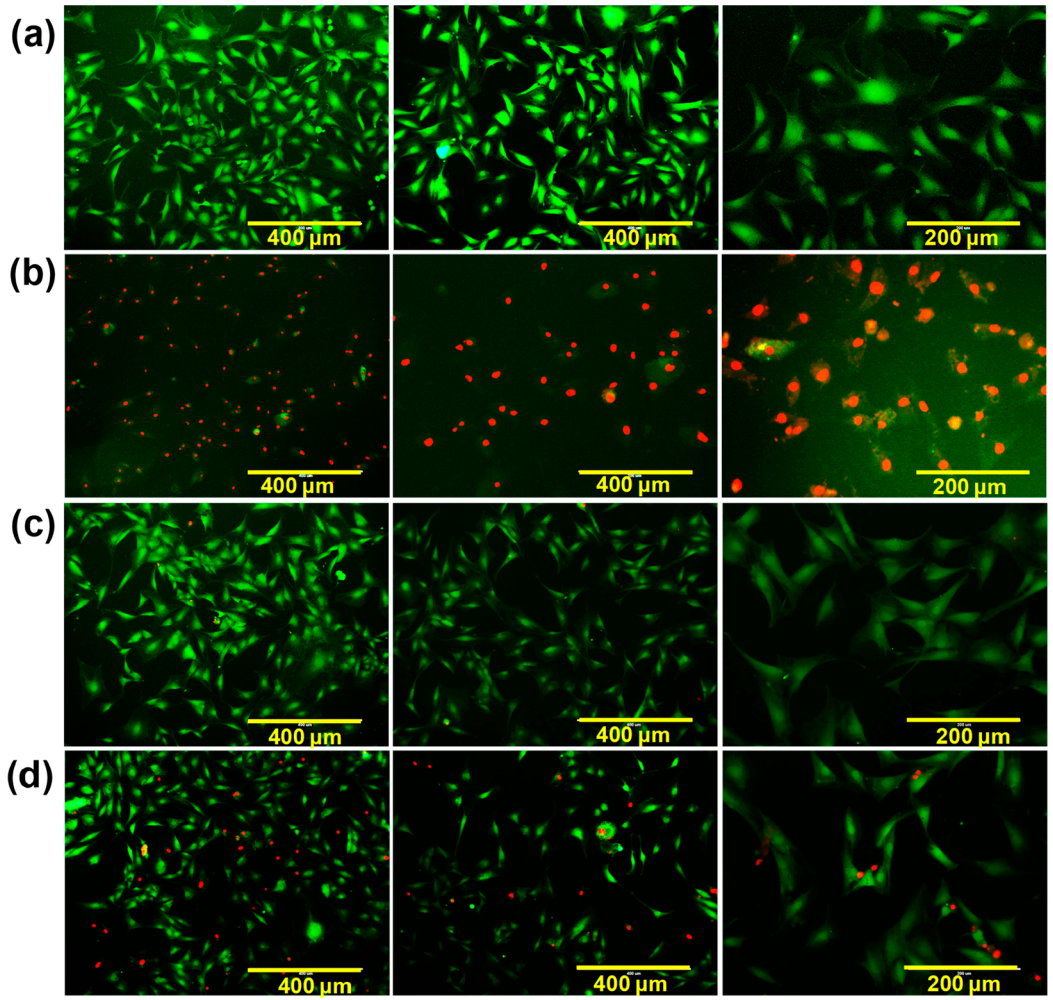

Figure 2. Fluorescence microscopy images demonstrating the effect of carbonates on the cytotoxicity produced by arsenate on IEC-6 cells at 3 ppm. Two different magnifications are shown for every type. Line (row) (a) Control cells without any treatment. Line (b) 3 ppm of As^{5+} treatment. Line (c) 3 ppm As^{5+} + 40 ppm of $CaCO_3$. Line (d) 3 ppm As^{5+} + 40 ppm of Na_2CO_3. Calcein stains the live cells green and ethidium bromide stains the dead cells red.

commonly used fluorescent tag that intercalates with nucleic acids and stains dead cells red. Figure 2 shows the effect of As on the IEC-6 cells and the increase in cell viability due to exposure to $CaCO_3$ and Na_2CO_3. The control IEC-6 cells showed only green fluorescence (Figure 2a), a characteristic of live cells, whereas 3 ppm As-treated cells showed significant red fluorescence, which indicated dead cells, as shown in Figure 2b. The cells treated with only 40 ppm of $CaCO_3$ or Na_2CO_3 showed a negligible number of dead cells (Supporting Information; Figures S1 and S2). Almost 75% of the cells of As^{5+} $CaCO_3$- or As^{5+} Na_2CO_3-treated samples were green fluorescent (Figure 2 c,d), indicating that carbonates protected IEC-6 cells from the As-induced cell death. The result was obtained from triplicate experiments. We observed that a cotreatment of carbonate showed effective protection against As-induced cell death. Due to the poor solubility of $CaCO_3$, precipitates were formed on the surface of the treated cells, as seen in the Supporting Information, Figure S1d. In order to understand if $CaCO_3$ is involved in As complexation,[26] SEM with EDS spectra and elemental maps of the $CaCO_3$ precipitates were studied (Supporting Information; Figure S3). Chemical characterization of the precipitates showed no presence of As on them, and thus, we infer that As−carbonate complexes might be of concentrations below the detection limit. Cyclic voltammetry experiments to study the effect of $CaCO_3$ on H_2O_2 concentration in the cells have shown 95% reduction in H_2O_2 concentration after incubation of IEC-6 cells with As^{5+} and 40 ppm of $CaCO_3$.

Morphological and Quantitative Assessment of Carbonate's Action. Morphological criteria have been used to define cell death. Rounded bodies observed in cell tissue culture are distinct morphological features associated with cell death (specifically, apoptosis) and cells under stress or exposed to stressful environments.[39] The untreated IEC-6 control cells were polygonal in shape with more regular dimensions and were grown attached to the substrate in discrete patches. Figure 3A shows the phase-contrast microscopic images of untreated control cells, cells treated with As^{5+}, As^{5+} + $CaCO_3$, and As^{5+} + Na_2CO_3 (Parts a, b, c, and d of Figure 3A, respectively). Morphological changes were observed in As-affected cells, whereas the cotreatment of As^{5+} with either calcium carbonate or sodium carbonate acted as a cytoprotectant and preserved the morphology similar to that of the control cells. The morphology of cells treated with 40 ppm of $CaCO_3$ or Na_2CO_3 was not disrupted (Supporting Information, Figure S4). $CaCO_3$-treated cells show increased

https://dx.doi.org/10.1021/acssuschemeng.9b06850
ACS Sustainable Chem. Eng. 2020, 8, 5067−5075

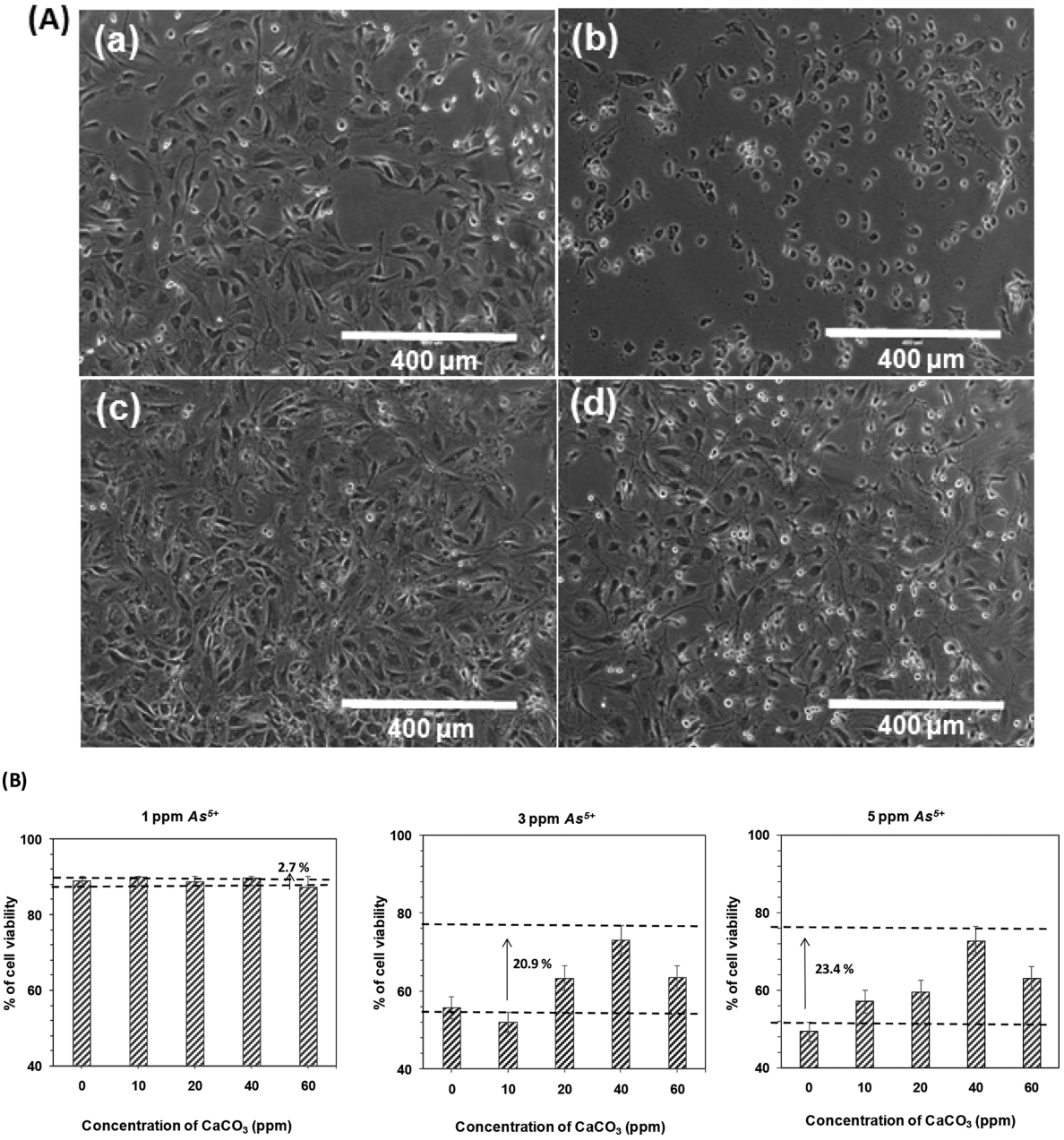

Figure 3. (A) Effect of arsenate on the cellular morphology and the cytoprotection by calcium carbonate and sodium carbonate. (a) Untreated control cells, (b) 3 ppm of As^{5+} treatment, (c) 3 ppm As^{5+} + 40 ppm of $CaCO_3$, and (d) 3 ppm As^{5+} + 40 ppm of Na_2CO_3. (B) Effect of calcium carbonate on the toxicity of varying concentrations of arsenate (As^{5+}). The percentage of cell viability was measured using MTT assay. The difference between the heights of dashed lines represents the increase in viability of the cells.

viability than Na_2CO_3-treated cells as the buffering capacity, and acid neutralization efficiency of $CaCO_3$ is higher than that of Na_2CO_3.[40]

This difference in viability was measured quantitatively using the MTT colorimetric assay. The cotreatment of the cells with a combination of As^{5+} + $CaCO_3$ (Figure 3B) or As^{5+} + Na_2CO_3 (Supporting Information, Figure S5) resulted in protection against As-induced toxicity in a dose-dependent manner. The cytosolic and mitochondrial dehydrogenases produced by the living cells reduced the yellow tetrazolium salt (MTT) and produced a purple formazan dye that was detected using a spectrophotometer. The viability of As-treated cells was restored to above 75% of the control when they were cotreated with carbonates. This cell viability assay stands as preliminary data to indicate the protective action of carbonate during As exposure. The total concentration of As in As^{5+} + $CaCO_3$-cotreated cells reduced by 31.5% when compared with the 3 ppm As^{5+}-treated cells (Supporting Information, Figure S6). In this study, we found that the concentration of carbonates above 10 ppm and below 40 ppm is necessary for protection.

Intracellular ROS Levels. An important biomarker to indicate oxidative stress caused by As is the intracellular level of ROS. When the ROS concentration increases, it indicates an increase in cellular oxidative stress. Initial experiments were performed with an oxidatively stressed model in which IEC-6 cells were treated with a toxic level of 3 ppm As. For a positive control to represent intracellular ROS production, cells were treated with 1 mM H_2O_2 for 1 h and were stained subsequently

https://dx.doi.org/10.1021/acssuschemeng.9b06850
ACS Sustainable Chem. Eng. 2020, 8, 5067−5075

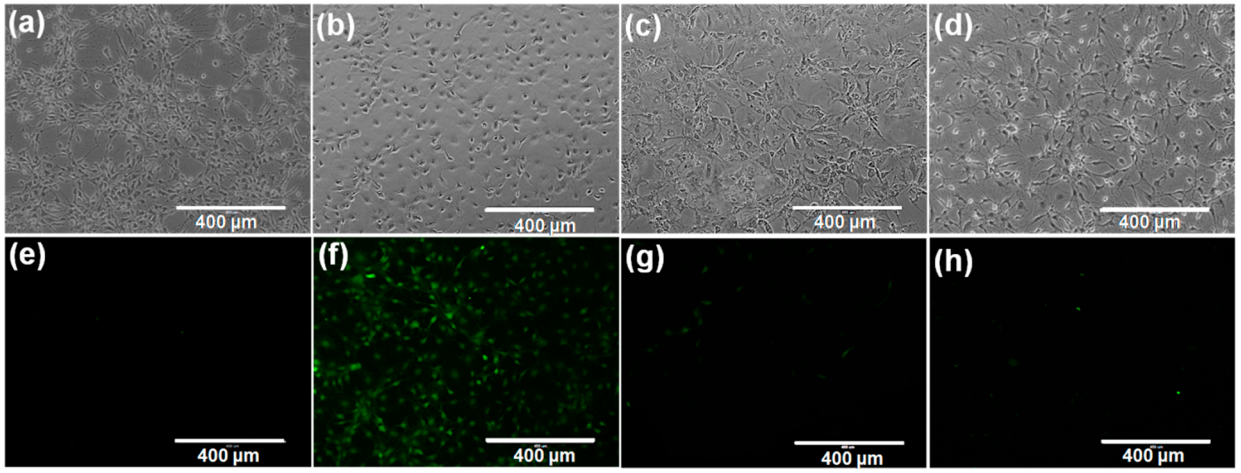

Figure 4. Determination of ROS in treated cells. Phase-contrast (top) and fluorescence microscopy (bottom) images demonstrating the effect of carbonates on the ROS produced by cells during 3 ppm As^{5+} treatment: (a, e) control, (b, f) 3 ppm As^{5+}, (c, g) 3 ppm As^{5+} + 40 ppm of $CaCO_3$, and (d, h) 3 ppm As^{5+} + 40 ppm of Na_2CO_3.

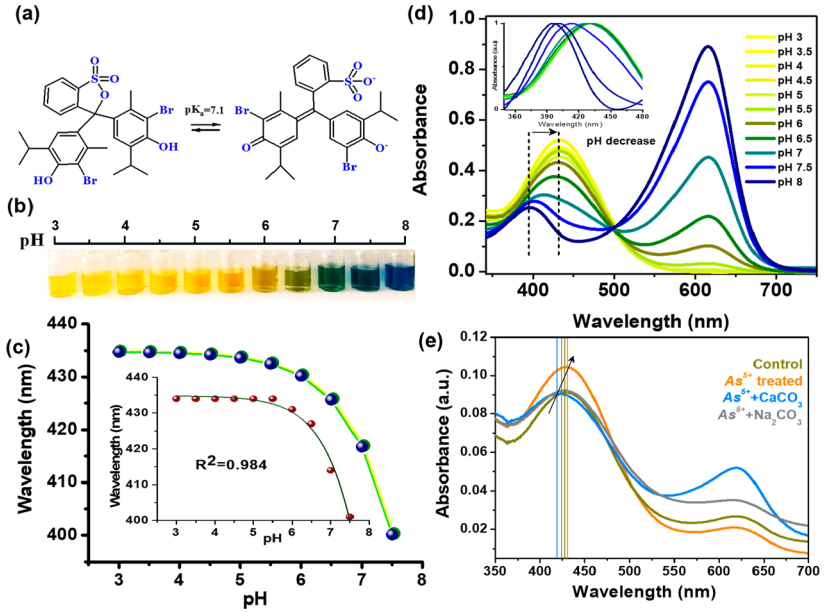

Figure 5. (a) Structure of BTB at different pH ranges. (b) Different colors of BTB at marked pH conditions. (c) Calibration curve of UV−vis absorption peak of the dye solutions. The inset shows the calibration curve from pH 4.5 to 7.5. (d) UV−vis absorption spectra of BTB/PBS solutions at different pH. The red shift in acidic solutions at 420 nm is marked. Inset is the normalized UV−vis absorption spectra in the 350−500 nm window at different pH. (e) UV−vis absorption spectra of the treated cells eluted from the culture plate, sonicated, and stained with BTB.

(Supporting Information, Figure S7). The As-treated cells showed green fluorescence depicting excessive oxidative stress (Figure 4f). The data summarized in Figure 4 show that the cotreatment of As^{5+} $CaCO_3$ or As^{5+} Na_2CO_3 (Figure 4g,h) significantly decreased the levels of intracellular ROS in comparison to that produced in As-treated cells. The negative control (untreated healthy cells) and 40 ppm of $CaCO_3$- (Figure 4e) or Na_2CO_3-treated cells showed no significant difference in the intracellular ROS production and showed no fluorescence. Parts a−d of Figure 4 are the phase-contrast images of control cells, cells treated with As^{5+}, 3 ppm As^{5+} + 40 ppm of $CaCO_3$, and 3 ppm As^{5+} + 40 ppm of Na_2CO_3, respectively. This experiment suggested that the protective role of carbonates is mediated, at least in part by direct H_2O_2 decomposition. The result was obtained from triplicate experiments for three separate trials. In all the experiments, treatment with carbonates resulted in a significant reduction in As-induced intracellular ROS production, proving its ability to decrease oxidative damage and subsequent cell death.

Cellular pH Profiling. Upon As^{5+} exposure, the acidic metabolites of As and the Warburg effect lead to a decreased pH in the cells. This was evident from the change in the color of the growth media (DMEM) in which As^{5+}-affected cells were cultured. Although the pH change in a cell is balanced by the buffering activity of the CO_3^{2-}/HCO_3^- system, the acidic metabolites formed due to As-induced toxicity were high in concentration, leading to cell death. Therefore, the effect of external administration of carbonates along with As^{5+} on the cellular pH was studied.

The UV−vis absorption spectra of the treated cells that were eluted from the culture plate, sonicated, and stained with BTB are shown in Figure 5. Each condition was tested in triplicate.

https://dx.doi.org/10.1021/acssuschemeng.9b06850
ACS Sustainable Chem. Eng. 2020, 8, 5067−5075

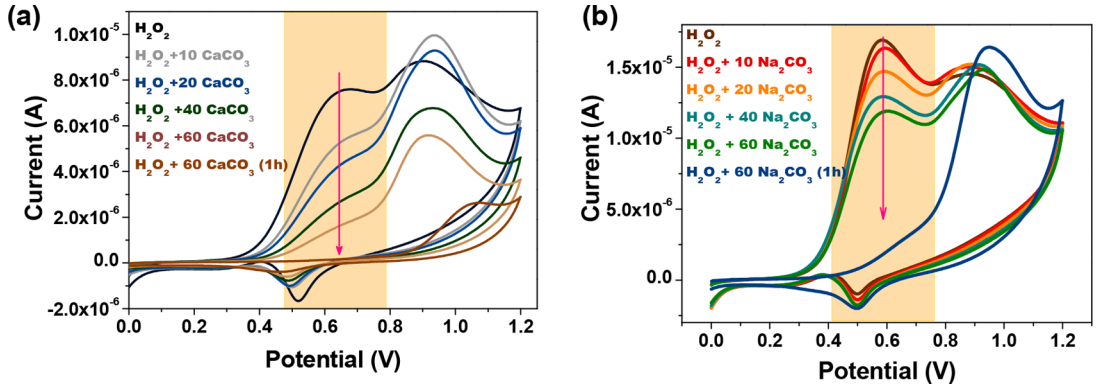

Figure 6. Carbonate's role in the decomposition of H_2O_2 at varying concentrations of (a) $CaCO_3$ and (b) Na_2CO_3 by cyclic voltammetry.

BTB can be in its protonated or deprotonated form, indicated by a yellow or blue color, respectively (Figure 5a,b). An intermediate of the deprotonation mechanism is responsible for a greenish color at neutral pH. The absorption spectra of BTB/PBS solution were initially studied at varied pH, and a correlation curve was obtained (Figure 5c) to quantitate and compare the pH of the treated cells. The dye shows two distinct features at 420 and 620 nm (Figure 5d). The protonated form of the dye had its peak absorption at 420 nm, thus transmitting yellow light in As^{5+}-treated acidic solutions, and the deprotonated form had its peak absorption at 620 nm, thus transmitting blue light in the control and carbonate-treated basic solutions (Figure 5e). This peak can be attributed to the occurrence of a hydrogen transfer (on the phenolic groups) and intramolecular charge transfer (caused by the conjugate effects of the system).

The color of BTB/PBS varies as an active indication of pH change in the range 6.0−7.6.[41] As the pH decreases in an As^{5+}-treated cell solution (the orange trace in Figure 5e), the highly pH-dependent absorption peak centered at 420 nm shows a definite red shift from 420 to 430 nm (inset of Figure 5d). The change in pH can be interpreted by comparing the peak center and the absorbance vs pH calibration curve plotted with standard solutions in the inset of Figure 5c, where the red shift reaches saturation thereafter. Another important feature is the absorption peak centered at 620 nm. This peak shown in the standard solution decreases gradually and finally disappears when the solution turns acidic. The peak intensity of the As^{5+}-treated cell solution (orange trace) at 620 nm had decreased significantly in comparison to that of the control cells. Whereas, there was an increase in the intensity of As^{5+} + $CaCO_3$-treated cells (blue trace) as the solution was neutralized.

A colorimetric imaging method with bright-field microscopy using a pH indicator, BTB, was used also to demonstrate the change in cellular pH. Upon optical microscopic observation, cells, when treated with 3 ppm of As^{5+}, stained yellow due to lowering of the cellular pH, whereas the color turned darker when treated with 3 ppm As^{5+} + 40 ppm of $CaCO_3$ and 3 ppm As^{5+} + 40 ppm of Na_2CO_3 (Figure S8a of Supporting Information). The pH distribution of treated cells was calculated from the calibration curve, which showed a decrease in the intensity of the 620 nm peak for As-treated cells, whereas the carbonate-treated cells retained the intensity similar to that of the control cells (Figure S8b of Supporting Information). The pH change of cotreated cells was 5−6.5, which was significant although being small. Treatment with carbonates balanced the cellular pH to the neutral range and prevented acid-promoted cellular stress.

H_2O_2 Decomposition. To prove that carbonates are efficient in decomposing H_2O_2 produced during oxidative stress induced by As^{5+}, a set of CV experiments were performed on As^{5+}-treated cells lysed in PBS. The CV curve of PBS (pH = 7) used in the experiment is shown in the Supporting Information, Figure S9. Figure 6 (a and b) shows the concentration-dependent decomposition of H_2O_2 through voltammogram when the cells were incubated for 1 min with calcium carbonate and sodium carbonate, respectively. In the potential window (0 ± 1.4 V), we observed a broad oxidation peak of H_2O_2 at 0.4−0.8 V. However, this peak gradually decreases with lowering of the concentration of H_2O_2 in the presence of carbonate in the sample. When the incubation time was increased, a complete decomposition was observed, which lead to the disappearance of the H_2O_2 peak. More than 95% reduction in H_2O_2 concentration was observed within an incubation period of 1 h. Studies on several different systems have demonstrated significant decomposition of H_2O_2 by carbonates.[42] It is reported that oxidative cell death in the presence of iron involves Fenton-type reactions, and peroxidative damage to the cell may be prevented by the decomposition caused by carbonates.[43]

In view of the above, the carbonate-mediated protection can be suggested due to one or more of the following mechanisms: (1) direct decomposition of ROS produced and (2) action as a buffering agent in neutralizing the acidic byproducts formed in the cell. The formation of As−carbonate complexes can be another mechanism, as reported in the literature.[44] Carbonated water may be a prudent solution in preventing the slow impairment caused by continuous intake of As from the contaminated water. The counteraction of carbonates on As toxicity has to be studied using animal models, and the influence of other metal ions in the digestive system on the effect of carbonate has to be investigated. Additional investigations on the impact of such measures on the overall well-being of individuals are necessary before proposing such methods as remedial measures.

CONCLUSION

Carbonates are nonhazardous, abundantly available in the earth's crust, and are affordable to all the communities present throughout the world. The current study shows that the administration of safe levels of carbonate in the form of calcium carbonate or sodium carbonate can counteract the toxicity levels of As. A cascade of cellular dysfunction that

https://dx.doi.org/10.1021/acssuschemeng.9b06850
ACS Sustainable Chem. Eng. 2020, 8, 5067−5075

occurs as a result of As toxicity results in cellular acidification and excessive ROS generation in IEC-6 cells. While acidification is neutralized by the buffering action of carbonates, the oxidative stress created inside the cell is counteracted by its H_2O_2 decomposing activity. Any mineral intake in living organisms through fluids plays a key role in maintaining its balance in comparison to food. We propose that a divided dose of mineral balanced water containing sodium carbonate and/or calcium carbonate at concentrations adjusted according to the As content can be the best way to compensate for the multiplex complications caused by As in the human system. While developing advanced materials to create an affordable drinking water purifier,[45] we have reported in our earlier work that 20−50 ppm of carbonates and other essential minerals can be released continuously and sustainably from confined scaffolds.[46,47] The use of such sustainable carbonate releasing encapsulations can provide cytoprotection against As toxicity at an affordable cost, without any energy demand. This paper stands as preliminary evidence to tackle the mass poisoning scenario by using this sustainable and affordable solution. Although the effective route of administration of carbonates in order to tackle As^{5+} contamination in living systems is not clearly understood in this study, this may be evaluated in the future by detailed clinical analysis.

■ ASSOCIATED CONTENT

Supporting Information

The Supporting Information is available free of charge at https://pubs.acs.org/doi/10.1021/acssuschemeng.9b06850.

Figures of fluorescence microscopy, phase-contrast microscopy, SEM, and bright-field optical microscopy images, EDS spectra, effects of Na_2CO_3 on the toxicity induced by varying concentrations, comparative analysis of As^{5+} concentration in cells, histograms of pH distribution, and CV curves (PDF)

■ AUTHOR INFORMATION

Corresponding Author

Thalappil Pradeep − *DST Unit of Nanoscience (DST UNS) and Thematic Unit of Excellence (TUE), Department of Chemistry, Indian Institute of Technology Madras, Chennai, Tamil Nadu 600036, India;* orcid.org/0000-0003-3174-534X; Email: pradeep@iitm.ac.in; Fax: +91-44-2257-0545

Authors

Swathy Jakka Ravindran − *DST Unit of Nanoscience (DST UNS) and Thematic Unit of Excellence (TUE), Department of Chemistry and Environmental and Water Resources Engineering (EWRE) Division, Department of Civil Engineering, Indian Institute of Technology Madras, Chennai, Tamil Nadu 600036, India;* orcid.org/0000-0002-7882-7871

Shantha Kumar Jenifer − *DST Unit of Nanoscience (DST UNS) and Thematic Unit of Excellence (TUE), Department of Chemistry, Indian Institute of Technology Madras, Chennai, Tamil Nadu 600036, India*

Jayashree Balasubramanyam − *Department of Nanobiotechnology, Vision Research Foundation, Sankara Nethralaya, Chennai, Tamil Nadu 600006, India*

Sourav Kanti Jana − *DST Unit of Nanoscience (DST UNS) and Thematic Unit of Excellence (TUE), Department of Chemistry, Indian Institute of Technology Madras, Chennai, Tamil Nadu 600036, India;* orcid.org/0000-0001-5772-7022

Subramanian Krishnakumar − *Department of Nanobiotechnology, Vision Research Foundation, Sankara Nethralaya, Chennai, Tamil Nadu 600006, India*

Sailaja Elchuri − *Department of Nanobiotechnology, Vision Research Foundation, Sankara Nethralaya, Chennai, Tamil Nadu 600006, India;* orcid.org/0000-0002-9780-2717

Ligy Philip − *Environmental and Water Resources Engineering (EWRE) Division, Department of Civil Engineering, Indian Institute of Technology Madras, Chennai 600036, India;* orcid.org/0000-0001-8838-2135

Complete contact information is available at: https://pubs.acs.org/10.1021/acssuschemeng.9b06850

Author Contributions

T.P. and S.J.R. designed the experiments. S.J.R. and J.B. performed the experiments. T.P., L.P., S.E., S.J.R. and S.K.J. analyzed the data and wrote the paper.

Notes

The authors declare no competing financial interest.

■ ACKNOWLEDGMENTS

The authors thank Mr. Ranjith and Mrs. Lakshmi for their timely support in cell culture, Mr. Srikrishnarka Pillalamarri for his technical support in SEM analysis, and the Science and Engineering Research Board (Government of India) for supporting this work through the grant, EMR/2015/000607, which made this research possible.

■ REFERENCES

(1) Straif, K.; Benbrahim-Tallaa, L.; Baan, R.; Grosse, Y.; Secretan, B.; El Ghissassi, F.; Bouvard, V.; Guha, N.; Freeman, C.; Galichet, L. A Review of Human Carcinogens-Part C: Metals, Arsenic, Dusts, and Fibres. *Lancet Oncol.* **2009**, *10* (5), 453−454.

(2) Toxicological Profile for Arsenic. Agency for Toxic Substances and Disease Registry. https://www.atsdr.cdc.gov/toxprofiles (accessed 2019-12-12).

(3) Paul, S.; Das, N.; Bhattacharjee, P.; Banerjee, M.; Das, J. K.; Sarma, N.; Sarkar, A.; Bandyopadhyay, A. K.; Sau, T. J.; Basu, S.; et al. Arsenic-Induced Toxicity and Carcinogenicity: A Two-Wave Cross-Sectional Study in Arsenicosis Individuals in West Bengal, India. *J. Exposure Sci. Environ. Epidemiol.* **2013**, *23* (2), 156−162.

(4) Ravenscroft, P.; Brammer, H.; Richards, K. *Arsenic Pollution: A Global Synthesis; RGS-IBG Book Series*; Wiley-Blackwell: UK, 2009.

(5) Occurence of high arsenic content in groundwater. India Environmental portal. http://www.indiaenvironmentportal.org.in (accessed 2019-12-23).

(6) Arsenic. WHO news room. https://www.who.int/news-room/fact-sheets/detail/arsenic (accessed 2019-11-05).

(7) Zhu, Y.-G.; Yoshinaga, M.; Zhao, F.-J.; Rosen, B. P. Earth Abides Arsenic Biotransformations. *Annu. Rev. Earth Planet. Sci.* **2014**, *42*, 443−467.

(8) Sreeprasad, T. S.; Maliyekkal, S. M.; Lisha, K. P.; Pradeep, T. Reduced Graphene Oxide−Metal/Metal Oxide Composites: Facile Synthesis and Application in Water Purification. *J. Hazard. Mater.* **2011**, *186* (1), 921−931.

(9) Yang, Q.; Lau, C. H.; Ge, Q. Novel Ionic Grafts That Enhance Arsenic Removal via Forward Osmosis. *ACS Appl. Mater. Interfaces* **2019**, *11* (19), 17828−17835.

(10) Hossain, M. A.; Sengupta, M. K.; Ahamed, S.; Rahman, M. M.; Mondal, D.; Lodh, D.; Das, B.; Nayak, B.; Roy, B. K.; Mukherjee, A.; et al. Ineffectiveness and Poor Reliability of Arsenic Removal Plants in West Bengal, India. *Environ. Sci. Technol.* **2005**, *39* (11), 4300−4306.

(11) Wang, J. S.; Wai, C. M. Arsenic in Drinking Water—A Global Environmental Problem. *J. Chem. Educ.* **2004**, *81* (2), 207−213.
(12) Sankar, M. U.; Aigal, S.; Maliyekkal, S. M.; Chaudhary, A.; Anshup Kumar, A. A.; Chaudhari, K.; Pradeep, T. Biopolymer-Reinforced Synthetic Granular Nanocomposites for Affordable Point-of-Use Water Purification. *Proc. Natl. Acad. Sci. U. S. A.* **2013**, *110* (21), 8459−8464.
(13) Kumar, A. A.; Som, A.; Longo, P.; Sudhakar, C.; Bhuin, R. G.; Gupta, S. S.; Anshup; Sankar, M. U.; Chaudhary, A.; Kumar, R.; et al. Confined Metastable 2-Line Ferrihydrite for Affordable Point-of-Use Arsenic-Free Drinking Water. *Adv. Mater.* **2017**, *29* (7), 1604260.
(14) Sudhakar, C.; Anil Kumar, A.; Bhuin, R. G.; Sen Gupta, S.; Natarajan, G.; Pradeep, T. Species-Specific Uptake of Arsenic on Confined Metastable 2-Line Ferrihydrite: A Combined Raman-X-Ray Photoelectron Spectroscopy Investigation of the Adsorption Mechanism. *ACS Sustainable Chem. Eng.* **2018**, *6* (8), 9990−10000.
(15) Ball, P. Arsenic-Free Water Still a Pipedream. *Nature* **2005**, *436* (7049), 313.
(16) Dixit, S.; Hering, J. G. Comparison of Arsenic(V) and Arsenic(III) Sorption onto Iron Oxide Minerals: Implications for Arsenic Mobility. *Environ. Sci. Technol.* **2003**, *37* (18), 4182−4189.
(17) Oberoi, S.; Barchowsky, A.; Wu, F. The Global Burden of Disease for Skin, Lung, and Bladder Cancer Caused by Arsenic in Food. *Cancer Epidemiol., Biomarkers Prev.* **2014**, *23* (7), 1187−1194.
(18) Vrijenhoek, E. M.; Waypa, J. J. Arsenic Removal from Drinking Water by a "Loose" Nanofiltration Membrane. *Desalination* **2000**, *130* (3), 265−277.
(19) Guo, H.-R.; Wang, N.-S.; Hu, H.; Monson, R. R. Cell Type Specificity of Lung Cancer Associated with Arsenic Ingestion. *Cancer Epidemiol. Biomarkers Prev.* **2004**, *13* (4), 638−643.
(20) Hughes, M. F. Arsenic Toxicity and Potential Mechanisms of Action. *Toxicol. Lett.* **2002**, *133* (1), 1−16.
(21) Jomova, K.; Jenisova, Z.; Feszterova, M.; Baros, S.; Liska, J.; Hudecova, D.; Rhodes, C. J.; Valko, M. Arsenic: Toxicity, Oxidative Stress and Human Disease. *J. Appl. Toxicol.* **2011**, *31* (2), 95−107.
(22) Flora, S. J. S.; Bhadauria, S.; Kannan, G. M.; Nutan, S. Arsenic Induced Oxidative Stress and the Role of Antioxidant Supplementation during Chelation: A Review. *J. Environ. Biol.* **2007**, *28* (2), 333−347.
(23) Liu, S. X.; Athar, M.; Lippai, I.; Waldren, C.; Hei, T. K. Induction of Oxyradicals by Arsenic: Implication for Mechanism of Genotoxicity. *Proc. Natl. Acad. Sci. U. S. A.* **2001**, *98* (4), 1643−1648.
(24) Shi, H.; Shi, X.; Liu, K. J. Oxidative Mechanism of Arsenic Toxicity and Carcinogenesis. *Mol. Cell. Biochem.* **2004**, *255* (1), 67−78.
(25) Vander Heiden, M. G.; Cantley, L. C.; Thompson, C. B. Understanding the Warburg Effect: The Metabolic Requirements of Cell Proliferation. *Science* **2009**, *324* (5930), 1029−1033.
(26) Kim, M.-J.; Nriagu, J.; Haack, S. Carbonate Ions and Arsenic Dissolution by Groundwater. *Environ. Sci. Technol.* **2000**, *34* (15), 3094−3100.
(27) Hochella, M. F.; Lower, S. K.; Maurice, P. A.; Penn, R. L.; Sahai, N.; Sparks, D. L.; Twining, B. S. Nanominerals, Mineral Nanoparticles, and Earth Systems. *Science (Washington, DC, U. S.)* **2008**, *319* (5870), 1631−1635.
(28) Sherman, T.; Chernova, M. N.; Clark, J. S.; Jiang, L.; Alper, S. L.; Nehrke, K. The Abts and Sulp Families of Anion Transporters from Caenorhabditis Elegans. *Am. J. Physiol. Physiol.* **2005**, *289* (2), C341−C351.
(29) Ruby, M. V.; Davis, A.; Schoof, R.; Eberle, S.; Sellstone, C. M. Estimation of Lead and Arsenic Bioavailability Using a Physiologically Based Extraction Test. *Environ. Sci. Technol.* **1996**, *30* (2), 422−430.
(30) Zhao, F.; Severson, P.; Pacheco, S.; Futscher, B. W.; Klimecki, W. T. Arsenic Exposure Induces the Warburg Effect in Cultured Human Cells. *Toxicol. Appl. Pharmacol.* **2013**, *271* (1), 72−77.
(31) Robey, I. F.; Baggett, B. K.; Kirkpatrick, N. D.; Roe, D. J.; Dosescu, J.; Sloane, B. F.; Hashim, A. I.; Morse, D. L.; Raghunand, N.; Gatenby, R. A.; et al. Bicarbonate Increases Tumor PH and Inhibits Spontaneous Metastases. *Cancer Res.* **2009**, *69* (6), 2260−2268.
(32) Navarro, J. A.; de la Rosa, M. A.; Roncel, M.; de la Rosa, F. F. Carbon Dioxide-Mediated Decomposition of Hydrogen Peroxide in Alkaline Solutions. *J. Chem. Soc., Faraday Trans. 1* **1984**, *80*, 249−253.
(33) Lithaw, P. N. *Glycolysis Regulation, Processes and Diseases*; Nova Biomedical Books: NY, 2009.
(34) Florence, T. M. The Production of Hydroxyl Radical from Hydrogen Peroxide. *J. Inorg. Biochem.* **1984**, *22* (4), 221−230.
(35) Maliyekkal, S. M.; Philip, L.; Pradeep, T. As(III) Removal from Drinking Water Using Manganese Oxide-Coated-Alumina: Performance Evaluation and Mechanistic Details of Surface Binding. *Chem. Eng. J.* **2009**, *153*, 101−107.
(36) Cumbal, L.; SenGupta, A. K. Arsenic Removal Using Polymer-Supported Hydrated Iron(III) Oxide Nanoparticles: Role of Donnan Membrane Effect. *Environ. Sci. Technol.* **2005**, *39* (17), 6508−6515.
(37) Litter, M. I.; Ingallinella, A. M.; Olmos, V.; Savio, M.; Difeo, G.; Botto, L.; Torres, E. M. F.; Taylor, S.; Frangie, S.; Herkovits, J.; et al. Arsenic in Argentina: Technologies for Arsenic Removal from Groundwater Sources, Investment Costs and Waste Management Practices. *Sci. Total Environ.* **2019**, *690*, 778−789.
(38) Mosmann, T. Rapid Colorimetric Assay for Cellular Growth and Survival: Application to Proliferation and Cytotoxicity Assays. *J. Immunol. Methods* **1983**, *65* (1), 55−63.
(39) Malek, A. M.; Izumo, S. Mechanism of Endothelial Cell Shape Change and Cytoskeletal Remodeling in Response to Fluid Shear Stress. *J. Cell Sci.* **1996**, *109* (4), 713−726.
(40) Kapil, N.; Bhattacharyya, K. G. A Comparison of Neutralization Efficiency of Chemicals with Respect to Acidic Kopili River Water. *Appl. Water Sci.* **2017**, *7* (5), 2209−2214.
(41) Hou, H.; Zhao, Y.; Li, C.; Wang, M.; Xu, X.; Jin, Y. Single-Cell PH Imaging and Detection for PH Profiling and Label-Free Rapid Identification of Cancer-Cells. *Sci. Rep.* **2017**, *7* (1759), 1−8.
(42) Cota, H. M.; Katan, T.; Chin, M.; Schoenweis, F. J. Decomposition of Dilute Hydrogen Peroxide in Alkaline Solutions. *Nature* **1964**, *203* (4951), 1281.
(43) Burg, A.; Shamir, D.; Shusterman, I.; Kornweitz, H.; Meyerstein, D. The Role of Carbonate as a Catalyst of Fenton-like Reactions in AOP Processes: $CO\dot{3}^-$ as the Active Intermediate. *Chem. Commun.* **2014**, *50* (86), 13096−13099.
(44) Han, M.-J.; Hao, J.; Christodoulatos, C.; Korfiatis, G. P.; Wan, L.-J.; Meng, X. Direct Evidence of Arsenic(III)-Carbonate Complexes Obtained Using Electrochemical Scanning Tunneling Microscopy. *Anal. Chem.* **2007**, *79* (10), 3615−3622.
(45) Swathy, J. R.; Udhaya, M. S.; Amrita, C.; Aigal, S.; Anshup; Pradeep, T. Antimicrobial Silver: An Unprecedented Anion Effect. *Sci. Rep.* **2015**, *4* (1), 1−5.
(46) Jakka Ravindran, S.; Mahendranath, A.; Srikrishnarka, P.; Anil Kumar, A.; Islam, M. R.; Mukherjee, S.; Philip, L.; Pradeep, T. Geologically Inspired Monoliths for Sustainable Release of Essential Minerals into Drinking Water. *ACS Sustainable Chem. Eng.* **2019**, *7* (13), 11735−11744.
(47) Swathy, J. R.; Pugazhenthiran, N.; Sudhakar, C.; Anil Kumar, A.; Pradeep, T. Sparingly Soluble Constant Carbonate Releasing Inert Monolith for Enhancement of Antimicrobial Silver Action and Sustainable Utilization. *ACS Sustainable Chem. Eng.* **2016**, *4* (7), 4043−4049.

https://dx.doi.org/10.1021/acssuschemeng.9b06850
ACS Sustainable Chem. Eng. 2020, 8, 5067−5075